Photonik
Ingenieurbüro
Dr. Walter Luhs

PE-0800
Holography

Table of Contents

1.0 The mystery of holography

When Gábor Dénes published his theories of holography in a series of papers between 1946 and 1951 he could not imagine that his work would lead to a wide filed of applications. To that times he had to work with light sources of low coherence length and in addition he use a in-line concept which showed beside the real image also a second image occurred which significantly disturbed the real image. Actually, he did not follow his ideas, disappointed from the poor quality. He was surprised when he came to know in 1959 about the success of Emmett Leith and Juris Upatnieks who succeeded in creating holograms with much better quality, since they used a two beam set-up instead of the one-beam in-line set-up of Gábor Dénes.
Already one year later the first laser has been demonstrated which suddenly bursts the holography.

Fig. 1: Emmett Leith and Juris Upatnieks (MSE EE '65) displayed their revolutionary laser transmission hologram of a toy train at the Optical Society's 1964 Spring Conference

From now on a powerful light source with a high coherence was available. In parallel a Russian scientist Juri Nikolajewitsch Denisjuk created his first hologram in 1958 based on the Lippmann's principle using a mercury lamp. In 1962 he significantly contributed with his famous "Denisjuk" hologram to the development of holography whereby he used only one beam (Fig. 54). His arrangement allows to create holograms which can be reconstructed without a laser. For all holograms is in common that for the creation a laser is needed. Since small and affordable laser are available the holography came also in the reach of hobbyists.

1.1 Coherence

In classic optics, light was described as coherent, if it could produce interferences. The term coherence was elaborated by the photon statistics introduced by quantum optics. It says that light is coherent when photons originate in the same phase cell, that is; they have the same frequency and phase within Heisenberg's uncertainty principle. Monochromatic light is only coherent if the partial waves also have the same phases.

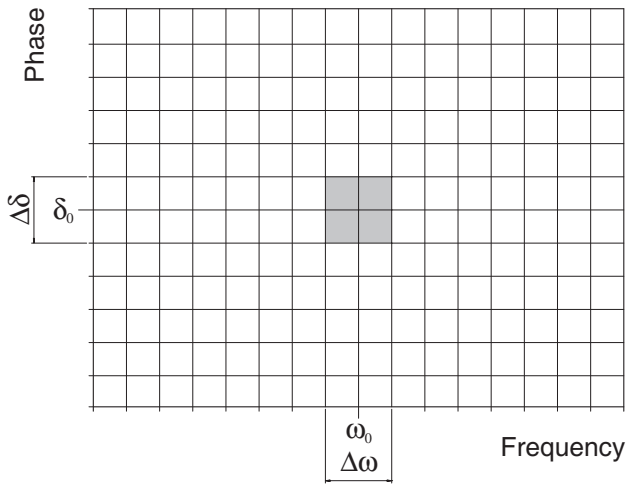

Fig. 2: Light, whose photons originate from the smallest possible phase cell according to Heisenberg's uncertainty principle, is coherent.

Classic optics states that light is coherent when it shows signs of interference. The narrower the emission line width Δω is, the higher will be the contrast observed in this process. There is obviously a connection between the contrast or visibility V of the interferogram and the line width of the light source used.

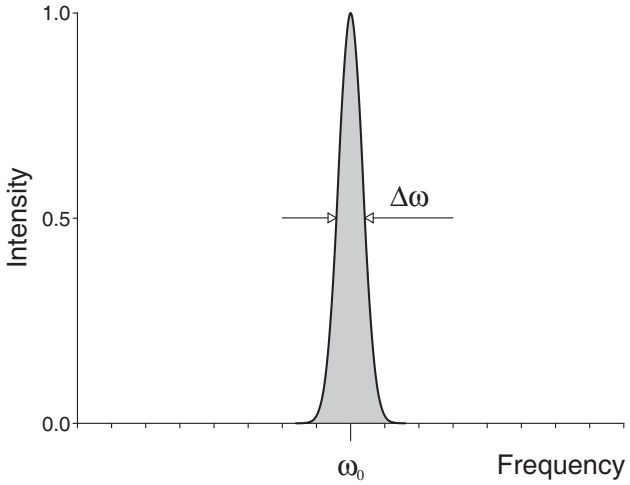

Fig. 3: Light with a narrow band emission with emission bandwidth Δω

If we follow the views of classic optics in the next chapters, this is because we will not touch the limits of Heisenberg's uncertainty principle by far, in spite of using a laser as the light source for the interferometer. The emission bandwidth and the emitted line width of the technical HeNe laser used is very wide compared to the theoretical natural bandwidth of a line.

1.2 Thermal light

We know from our daily observations that a hot body transmits light radiation. The higher the temperature of the body, the whiter the light seems.
It can thus be concluded that this kind of radiator has a very large emission bandwidth Δω. Therefore thermal light sources are not suitable for interferometry.

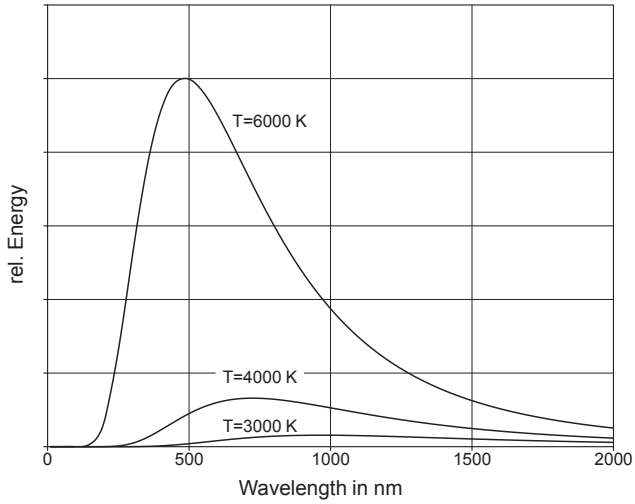

Fig. 4: The spectral distribution of a black body radiator (thermal radiator, Planck's radiation law) for various temperatures

1.3 Cold light

Another type of light production is the light emission of atoms and molecules, which show a clear spectral structure characteristic of certain atoms, and molecules, contrary to the continuous radiation of the temperature radiators. Apart from their characteristics as a light source, the main interest in spectra was to use them to find out more about the structure of atoms and molecules.

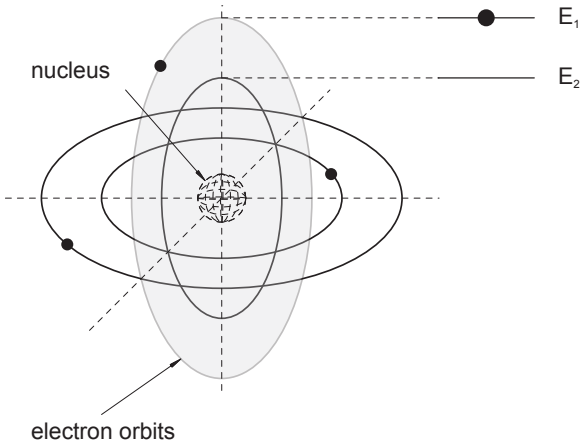

Fig. 5: Bohr's idea of the atom

Einstein elaborated Bohr's' theories on the atom model to the extent that light emitted or absorbed from the atoms can only have energies of E_2-E_1=hν (Fig. 5). His work and measurements proved that both in a resonant cavity and in the case of atomic emission discrete energies must be assumed. Einstein started off by trying to find one single description for these two types of light sources. He found the solution to this problem in 1917 when he derived Planck's hypothesis once more in his own way. Photons or a radiation field are produced through the transition from 2 → 1. Regarding to what we have already considered, the frequency of the radiation produced in this way should actually be determined by E_2-E_1 = h ν_0. However, keeping in tune with Heisenberg's uncertainty principle

$$\Delta x \cdot \Delta p_x \geq \frac{1}{2}\hbar \quad \text{or} \quad \Delta E \cdot \Delta t \geq \frac{1}{2}\hbar \,,$$

which states that every emission process is affected by an uncertainty and the emission line therefore always has a certain width Δω.

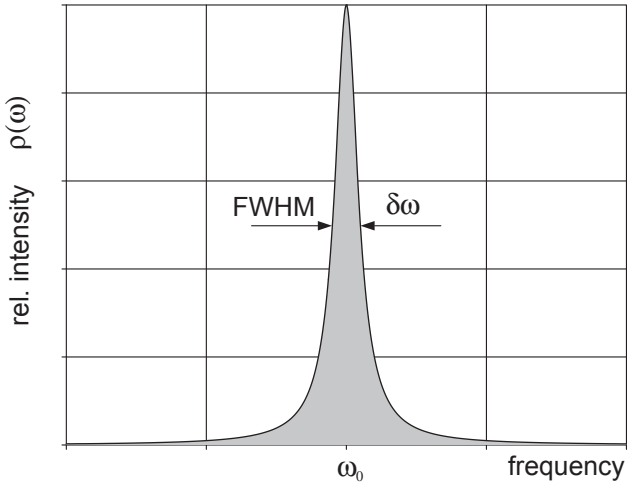

Fig. 6: Natural line width

$$\rho(\omega) = \frac{1}{(\omega - \omega_0)^2 + (1/2 \cdot \tau_s)^2}$$

This type of curve represents a Lorentz curve. Here, ω_0 is the resonant frequency and

$$\tau_s = \frac{1}{A_{21}}$$

is the average life of state 2. The half-width value δω (or also FWHM, Full Width at Half Maximum) of the curve according to Fig. 6 is calculated by inserting the value for ρ(ω) = 1/2. We find that

$$\delta(\omega)_{nat} = A_{21} \qquad (1.7.1)$$

the natural line width of a transition, defined by the Einstein coefficient A_{21}, which has a particular value for every transition. The results gained can also be interpreted to mean that state 2 does not have any sharply defined energy but an expansion with a half-width value of $\Delta E = 2\,\pi\,h\,A_{21}$. There would therefore be some uncertainty in this state. Quantum mechanics has shown that this effect is of fundamental importance. It has been called the Heisenberg's uncertainty relation after its inventor. In normal optical transitions, the value of τ_s is between 10^{-8} and 10^{-9} sec. This lifetime, determined by the spontaneous transitions alone is a decisive factor for the so called natural half-width value of a spectral line. Regarding descriptions, it must be stressed at this point that we must differentiate between the width of a state and the width of a line as well as between the terms state and line. Atomic states always exist, so no statement will be made on whether the state is occupied or empty. A line can only be formed if, for example, an emission occurs by the transition from the state from to 2→1. The line is a word used by spectroscopists. They may produce, for example, photographic plates using their spectral apparatus, on which fluorescent light is shown divided up into its wavelengths. They use slits in the optical radiation path for an easy evaluation of the spectra. Fig. 7 shows this kind of line spectrum.

Fig. 7: Photograph of the emission of a light source with the corresponding energy level showing a commonly known line spectrum.

The spectrum according to Fig. 7 can be seen from the line widths as well as from the emission wavelengths. Please note, however, that the measurement apparatus makes the line widths appear larger than they are.
If the spectral distribution of a line radiator were carried into that of the thermal radiator, the result would be a narrower line than the one in Fig. 4.
Let us return to the influence of the spectral bandwidth Δω on the contrast of our interferometer. To make it easier we have selected the intensities as

$$I_{01} = I_{02} = \frac{1}{2} \cdot I_0$$

and obtain for the intensity of the interfering waves:

$$I = I_0 \left\{1 + \cos\left(k \cdot \Delta L\right)\right\}.$$

However, now the intensity I_0 is a function of ω:

$$I_0 \rightarrow \hat{I}(\omega) = \hat{I} \cdot \rho(\omega) \cdot \partial\omega$$

So, we must integrate over all ω:

$$I = \int_{-\infty}^{+\infty} \left\{\hat{I} \cdot \rho(\omega) + \hat{I} \cdot \rho(\omega) \cdot \cos\left(\omega / c \cdot \Delta L\right)\right\} \cdot \partial\omega$$

and obtain for the interferogram:

$$I = I_0 + \int_{-\infty}^{+\infty} \hat{I} \cdot \rho(\omega) \cdot \cos\left(\omega / c \cdot \Delta L\right) \cdot \partial\omega \qquad (1.7.2)$$

We can obtain the contrast or the visibility of the interference from the extreme values of (1.7.2):

$$V(\Delta L) = \frac{I_{max} - I_{min}}{I_{max} + I_{min}}$$

Thus, the contrast function V, which is still dependent on ΔL after the integration, is the envelope of the interferogram I(ΔL). According to the form the emission line takes, or how the function ρ(ω) is made up, we can obtain the contrast of the function of the path difference ΔL and the corresponding contrast function V(ΔL) by using the above integration. The emission line of the laser, which we will use in the later experiment, can be described using a Gaussian function with a bandwidth Δω. The integral according to (1.7.2) can be calculated in this way. The calculation is carried out in [1] and the contrast function is shown in the following diagram.

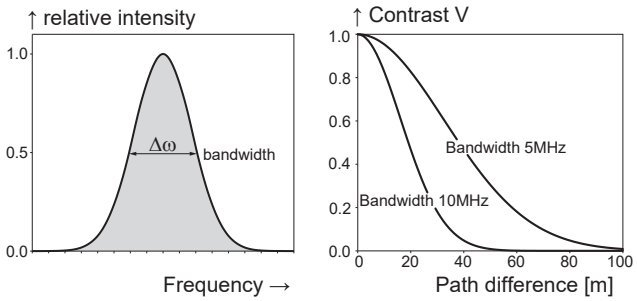

Fig. 8: Contrast as a function of the path difference of a light source with an emission bandwidth of 5 or 10 MHz (Laser).

The diagram on the right-hand side of Fig. 8 shows the contrast function. It shows that the contrast in a Gaussian distribution curve gradually drops as the path difference between both interfering waves increases. Theoretically, if the path difference is infinitely long, the contrast will eventually be zero. However, this is not a practical answer. Although technical interferometers are being used for a long time there is no information on a marginal contrast, which merits an evaluation. We have therefore taken the liberty of defining the marginal contrast ourselves. We would say that if the contrast V has dropped to

$$\frac{1}{e^2} \cdot V_{max} \approx 0{,}14$$

the practical coherence length Le has been reached. Since these associations are important, we should now examine the practical conditions in more detail in anticipation of the experiments that are still to come.
During our studies, we had taken a partial ray from a ray of light at a location situated at any given distance from a light source. We will give the coordinate Z_1 to this location. Another partial ray is taken from a second location with the coordinate Z_2. Both the partial rays are joined together, and the intensity of the superimposed ray is measured.

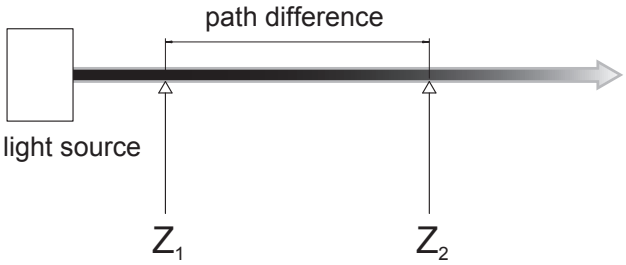

Fig. 9: Definition of coherence time

The photons taken from location z_2 must travel a longer path than the photons at location z_1. Since all photons fly at the speed of light c, the photons at location z_2 must have been "born" earlier than those at z_1. The time difference between both photon generations is obviously

$$\Delta t = \frac{\Delta L}{c}$$

If we choose a path difference ΔL, that is large enough to cause a drop in contrast to the value we defined, then the corresponding running time Δt will be known as the coherence time. We have introduced this term for didactic reasons. It is not required in our further observations. The construction according to Fig. 9 has a considerable disadvantage in that it cannot be carried out practically. The simplest basic form of a regulatory device for interference is the Michelson

interferometer. Although the physical situation we have just discussed is the same, the path difference must be observed more closely.

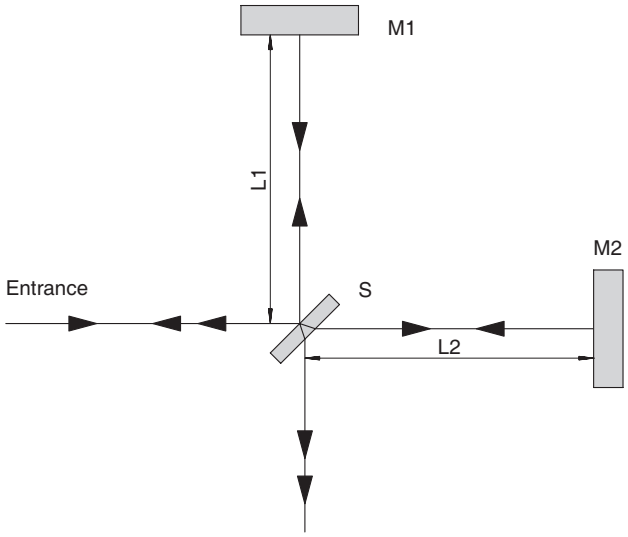

Fig. 10: Calculating the path difference DL using the Michelson interferometer

The beam splitter S splits the incoming beam. This is the origin of our system of coordinates. The mirror M1 should always be static, whereas the mirror M2 should be movable. Thus, the two radiation paths form two arms of the interferometer. The one with the static mirror is known as the reference arm and the one with the movable mirror is the index arm. The partial beam in the reference arm travels a path of 2 L1 before it returns to the reunification point at the beam splitter S. The path 2L2 is crossed in the reference arm. The path difference is therefore:

$$\Delta L = 2 \cdot \left(L_2 - L_1 \right)$$

We assume that the thickness of the beam splitter plate is zero. If $L_2 = L_1$, the path difference is zero. This can be adjusted for any number of intervals between the mirrors. In this state, the Michelson interferometer is symmetrical and even white light produces an interference pattern. This type of interferometer is sometimes also known as a white light interferometer. To find out the coherence length of the light source, the path difference is increased by shifting the mirror M2. There should be no maladjustment while doing this since this will also reduce the contrast. If we measure this contrast as a function of the path difference, we get the contrast function. The point, at which the contrast is below the value already given by us, is the point where the coherence length has been reached. The following interference patterns would probably be seen on a screen.

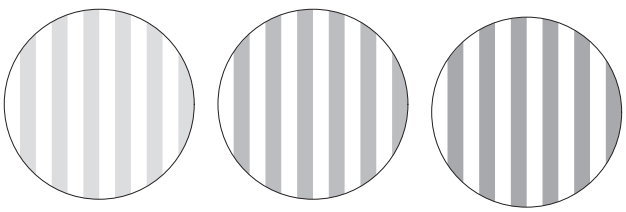

Fig. 11: Decreasing contrast with an increase in path difference.

Michelson carried out his experiments with the red line of a cadmium lamp that had a coherence length of only 20 cm. Since the index arm is crossed twice he had a measurement area of only 10 cm at his disposal. By measuring the contrast function, it is possible to find out the line width of the light source with (1.7.2). Can you imagine that Michelson carried this out with the green Hg line and saw 540,000 wavelengths in path difference with his naked eye, Perot and Fabry saw 790,000 and Lummer and Gehrcke as much as 2,600,000! Try and picture this process: The shifting of the measurement reflector, observing the light and dark band with the naked eye and counting to 2,600,000 at the same time. Till now we have examined the situation where the light source has different emission bandwidths but only one individual emission line. If we use a laser as a light source, the emission can consist of several so called 'longitudinal oscillation modes', as long as we do not take specific measures to produce only one.

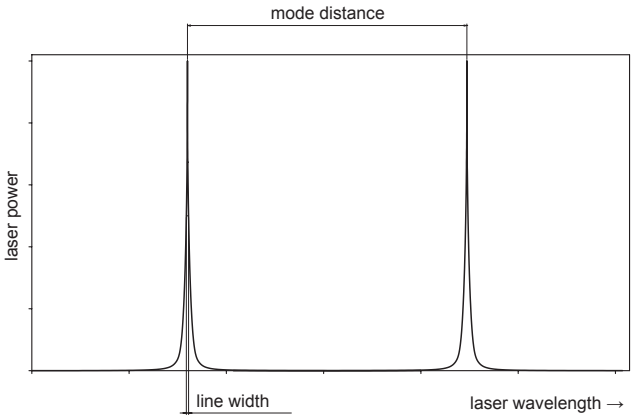

Fig. 12: Emission spectrum of the two-mode HeNe laser used

The expected interferogram will consist of a superimposition of the waves with both the frequencies ω and δω.

$$I = I_0 \cdot \left\{ 1 + \frac{1}{2} \cos\left(\frac{\omega}{c} \cdot \Delta L \right) + \frac{1}{2} \cos\left(\frac{\omega + \delta\omega}{c} \cdot \Delta L \right) \right\}$$

We can form a picture of the contrast function without having to make an explicit evaluation of the integral according to (1.7.2) by discussing the interferogram for some values of DL, using

$$\cos\alpha + \cos\beta = 2 \cdot \cos\left(\frac{\alpha + \beta}{2} \right) * \cos\left(\frac{\alpha - \beta}{2} \right)$$

$$I = I_0 \left\{ 1 + \cos\left(\frac{2\omega + \delta\omega}{2c} \cdot \Delta L \right) \cdot \cos\left(\frac{\delta\omega}{2c} \cdot \Delta L \right) \right\}$$

Since $\omega >> \delta\omega$

$$I = I_0 \left\{ 1 + \cos\left(\frac{\omega}{c} \cdot \Delta L \right) \cdot \cos\left(\frac{\delta\omega}{2c} \cdot \Delta L \right) \right\}$$

Since δω is not dependent on ω, this term is constant as far as the integration of all wavelengths is concerned and the contrast function of the single mode emission $V_1(\Delta L)$ becomes:

$$V_2(\Delta L) = V_1(\Delta L) \cdot \cos\left(\frac{\delta\omega}{2c} \cdot \Delta L \right)$$

The contrast function resulting from the two-mode emission is reproduced by the single mode emission, but the periodicity δω/2 superimposes with the cosine. The contrast is therefore zero for

$$\frac{\delta\omega}{2\cdot c}\cdot\Delta L=(2n+1)\cdot\frac{\pi}{2}\text{ , n = 0,1,2 ....}$$

or

$$\Delta L=(2n+1)\cdot\frac{c}{\delta\omega}.$$

The intervals between the zero points is exactly

$$\Delta L=\frac{c}{2\cdot\delta\nu}.$$

Let us remind ourselves of the interval in frequencies of longitudinal modes of a laser resonator:

$$\delta\nu=\frac{c}{2\cdot L}.$$

In this case L is the interval between the laser mirrors, so the interval between the zero points of the contrast corresponds exactly to the resonator length of the two-mode laser used.

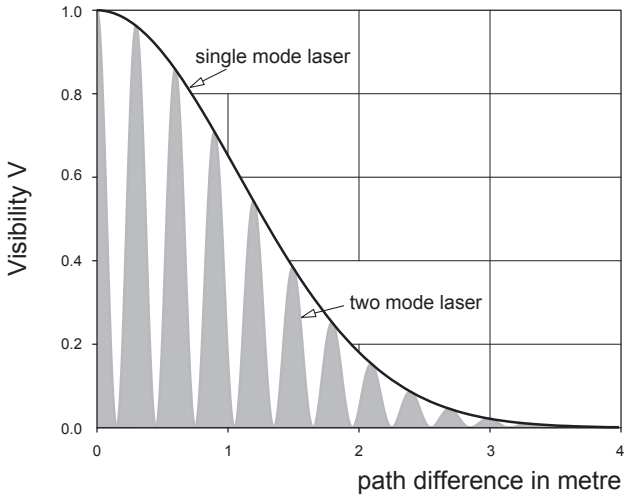

Fig. 13: Contrast as a function of the path difference of a single mode and a two-mode laser

Although the radiation is coherent, there is a disappearing contrast. In this case, it is not due to a lack of coherence, but to the phenomenon of optical interference. If the laser emission is put onto a photodetector at a suitably fast speed, we will have direct proof of optical interference. Optical interference can be demonstrated using an oscilloscope or a spectrum analyser. However, this would mean that when a two-mode laser is used in interferometry the available measurement area of the index arm would be limited to L/2. Although the contrast does increase when this value is exceeded there is no information available during the zero crossings.

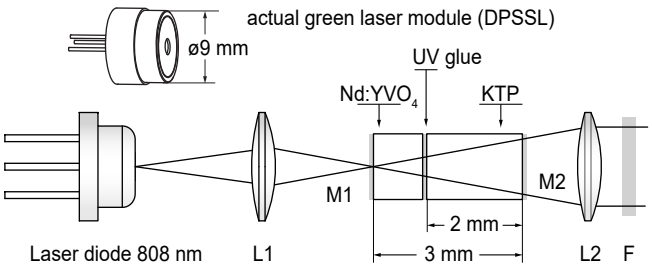

Fig. 14: Diode pumped solid state laser (green laser pointer)

The DPSSL has a cavity length of 3 mm consisting of the diode pumped Nd:VO₄ and a KTP crystal for frequency doubling. Lenses L1 and L2 focus the pump and collimate the frequency doubled radiation. All components are assembled in a housing of about 15 mm length and 9 mm diameter.
For the holography experiments here, a standard frequency doubled diode pumped Nd:YVO₄ laser (Fig. 14) emitting at 532 nm with an output power of about 100 mW is used. The compact compound of the Nd:YVO₄ and the attached KTP crystal together with the pump diode are mounted on an actively cooled metal heat sink with a Peltier element and operated with a stabilized power supply. The mirrors M1 and M2 form the cavity for the fundamental radiation at 1064 nm and are coated for highest reflectivity for this wavelength. In addition, M1 has a high transmission for the pump radiation at 808 nm and a high reflectivity for the second harmonic at 532 nm, while M2 has a high transmission for the second harmonic. The filter F is used to suppress any residual radiation either at 808 nm or 1064 nm. Considering the index of refraction for YVO₄ and KTP the optical cavity length is 5.4 mm, resulting in a spectral mode distance of the fundamental mode of about 28 GHz. The gain bandwidth of the Nd:YVO₄ crystal is 0.96 nm at 1064 nm or 254 GHz, allowing about 9 modes to oscillate. In principle each fundamental mode may create a second harmonic if the phase matching requirements are fulfilled. However, due to the mainly homogeneously broadened gain profile, single frequency emission is expected.

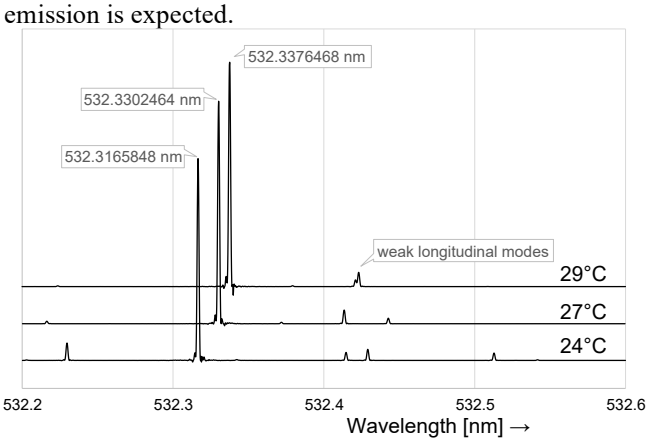

Fig. 15: Spectrum of the DPSSL for different temperatures, taken with a high-resolution Fourier spectrometer Spectrum of the DPSSL for different temperatures, taken with a high resolution Fourier spectrometer

Indeed, performed measurements with a Fourier spectrometer (Fig. 15) and a scanning Fabry-Perot (Fig. 16) indicate oscillation of only one strong mode, accompanied sometimes by very weak additional modes (Fig. 15), which may occur due to residual inhomogeneously broadened parts of the gain profile.

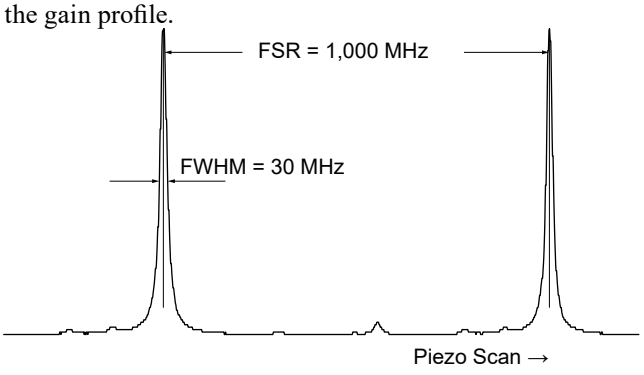

Fig. 16: Mode spectrum of the DPSSL taken with a confocal scanning Fabry Perot (SFP). Mirror radii of curvature 75 mm; resulting free spectral range (FSR) 1000 MHz.

In Fig. 15 the emission spectrum of the DPSSL for different temperatures is given, taken with a high-resolution Fourier spectrometer. Narrow single line emission is clearly seen, with some weak side emissions at distances of about 0.1 nm from the main emission. From the measurements a temperature tuning coefficient of 0.004 nm/°C or 4.45 GHz/°C is obtained.

The Fourier spectrometer allows absolute wavelength measurements, but it cannot resolve the spectral emission width of the emission. To get a better information of the emission width, a spherical scanning Fabry-Perot, consisting of two mirrors with radii of 75 mm at a distance of 75 mm (confocal resonator), having a finesse of about 33, was used. Fig. 16 shows a typical mode spectrum, indicating single frequency emission with a spectral width of less than 30 MHz. However, this width is limited by the resolution of the Fabry-Perot. For comparable all solid state laser systems linewidths well below 100 KHz have been measured. Assuming a linewidth of 100 kHz the coherence length L amounts to stunning

$$L = \frac{c}{\delta\nu} = 3.000\,\mathrm{m}$$

Even though such a coherence length is by far not required, the DPSSL has to be temperature controlled and stabilized to avoid mode jumping or wandering.

2.0 Principle of Holography

The basic concepts of holography are interference and the structure of wave fronts emerging from an object. For this we need to understand firstly the Huygens's and secondly the Huygens Fresnel principle.

2.1 Huygens principle

Fig. 17: Christiaan Huygens (1629 -1695)

In 1678 the great Dutch physicist Christian Huygens published a his "Traite de la Lumiere" on the wave theory of light. In his work he stated that the wave front of a propagating wave of light can be considered as the envelope of spherical wavelets emanating from every point on the wave front at the previous one.

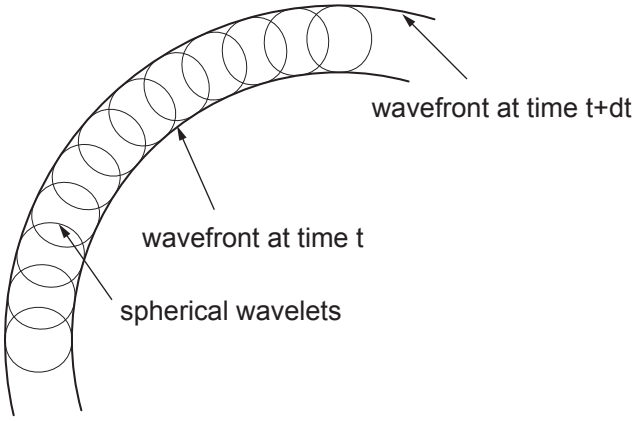

Fig. 18: Huygens principle

The wavelets have the same speed as the overall wave. His idea is shown Fig. 18 and became generally known as "Huygens Principle".

Fig. 19: Augustin-Jean Fresnel 1788 – 1827

Fresnel added to Huygens principle the idea that the amplitudes of the individual wavelets are summarized and forming a new wave front.

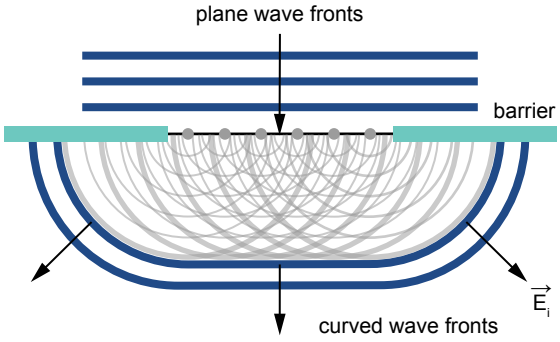

Fig. 20: Huygens and Fresnel principle shown at an aperture

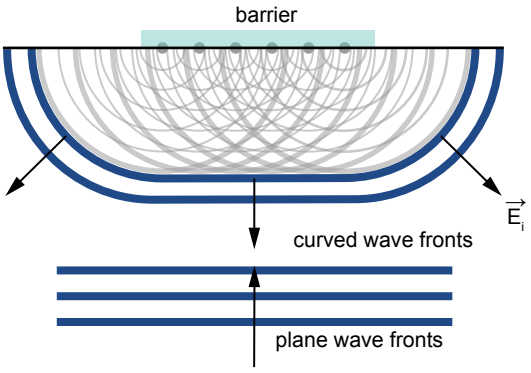

Fig. 21: Inverse aperture

Each location of the surface of a body can be considered as starting point of wavelets. The wavelets are creating a specific wave front. Parts of such a wave front are entering our

eyes and we can “see” the object.
If we would be able to create the same wave front let us say by some physical tricks, we also have the impression that we see the object.
This is what a hologram does. Firstly, we record the wave fronts of an object. That means we need to store the vectorial distribution of the electrical field E of the light which is emitted from the object.
Secondly, we need a possibility to “replay” or reconstruct the hologram, which means that the hologram shall provide actively the same wave fronts enabling us to see the impression of the recorded body.

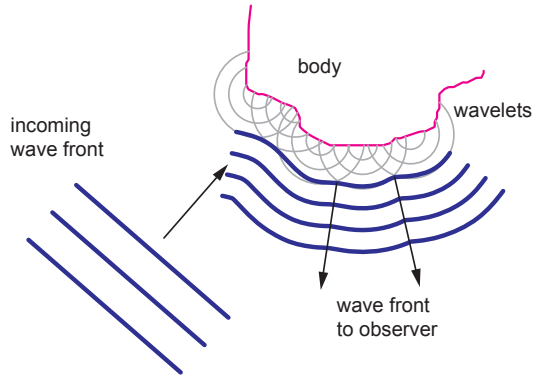

Fig. 22: Common situation of monitoring or recording of an illuminated object

The situation shown in Fig. 22 demonstrated the simple “photographing” of the body. We store only the intensity distribution and no spatial information.

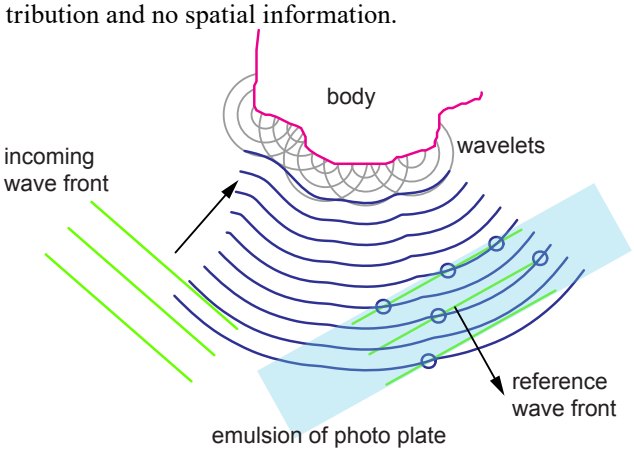

Fig. 23: Adding a reference wave front

We are using now coherent light for the illumination of the object. To obtain the spatial information the object waves are superimposed by a reference wave with the same spectral properties as the illuminating wave front.
In practice the light comes from one light source whereby the two beams are created by beam splitter in such a way that both beams maintain the same spectral and phase properties.
The resulting interference pattern is related to an intensity distribution which is stored inside the emulsion of a photo plate.

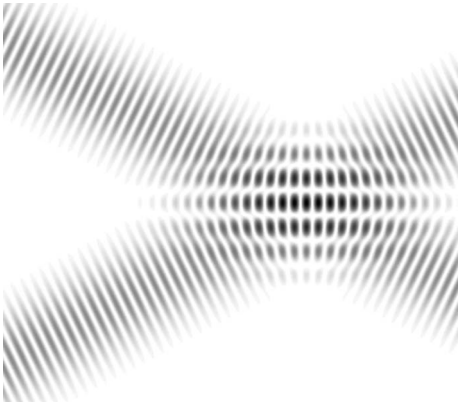

Fig. 24: Interference pattern of two crossing plane waves

The example of Fig. 24 shows the interference pattern or intensity distribution of two crossing plane waves.

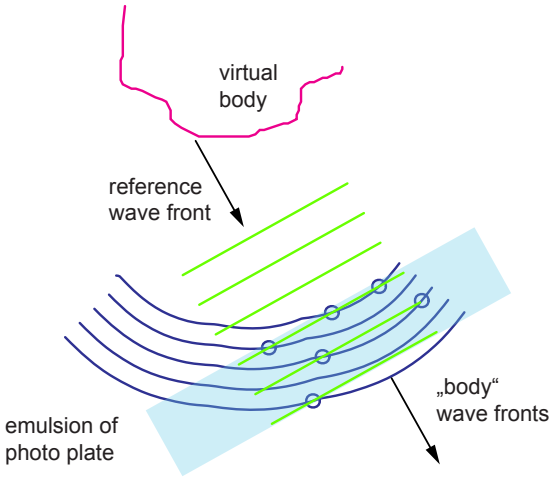

Fig. 25: Reconstruction of the hologram

The reference light is diffracted at the interference structure inside the emulsion of the photo plate in such a way that wave fronts are created and formed which are identically as if they would emerge from the body.

Theory

3.0 Experimental set-up

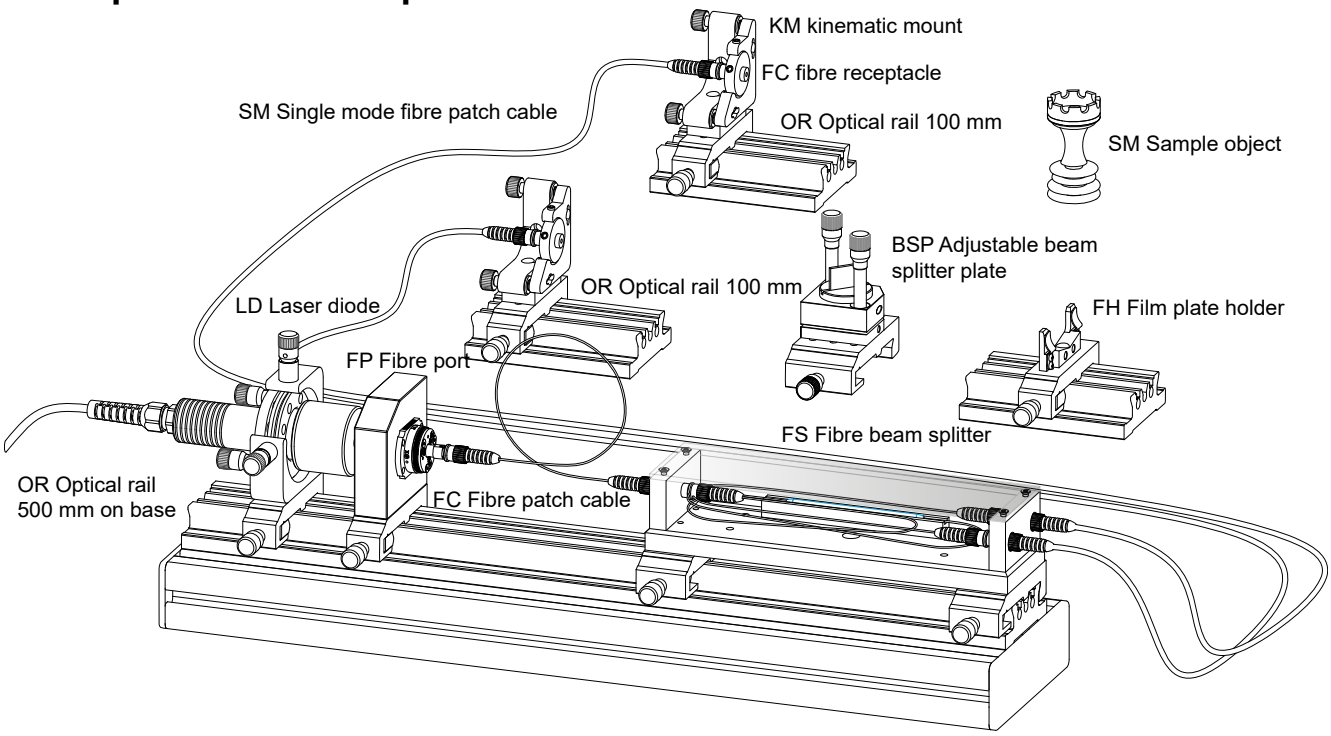

Fig. 26: PE-0800 Holography set-up

3.1 Description of the modules

3.1.1 Laser module (LD)

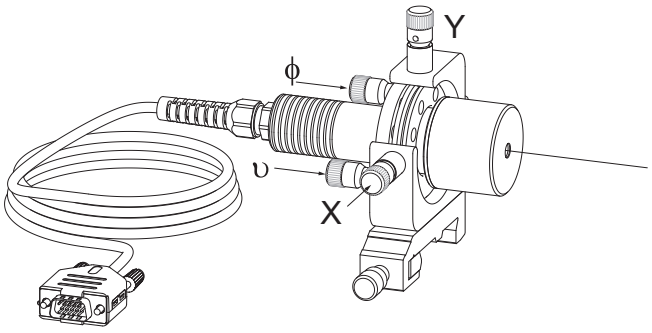

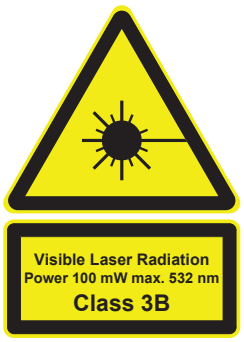

Fig. 27: Laser module LD

The laser module consists of a DPSSL (Diode Pumped Solid State Laser) with second harmonic generation and can emit 100 mW at 532 nm. The module is mounted into a 4 axis adjustment holder and is controlled by the timer and controller device DC-0090.

Caution:

If no measures can be taken to avoid direct looking into the laser beam, the user should wear suitable laser safety goggles.

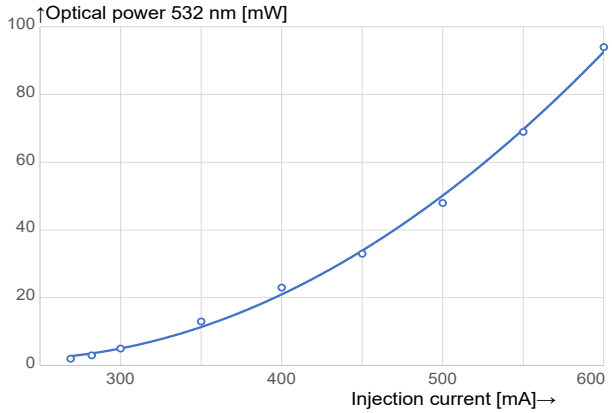

Fig. 28: Laser power versus injection current

The laser module consists of diode pumped Nd:YAG laser operating at 1064 nm with frequency doubling to 532 nm. In Fig. 28 the power of the frequency double radiation at 532 nm as function of the injection current of the pump diode. The typical quadratically relation can be recognised.

The emitted laser beam is fed into an optical single mode fibre with a core diameter (2a) of 3 µm.

3.1.2 Fibre coupling

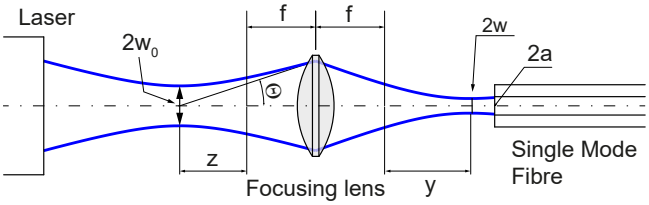

Fig. 29: Coupling laser light into a single mode fibre

For this purpose, a precise coupling element is needed which contains beside the focusing lens high precision actuators for tilting and shifting the focusing lens.

The radius *w* at the waist is:

$$w = \frac{w_0 \cdot f \cdot \theta \cdot}{\sqrt{w_0^2 + \theta^2 \cdot z^2}}$$

The position of the waist is:

$$y = \frac{z \cdot f^2}{z^2 + \left(\frac{w_0}{\theta}\right)^2}$$

By using the above equations, the characteristic parameter can be calculated and it becomes clear, that a precise adjustable component is required.

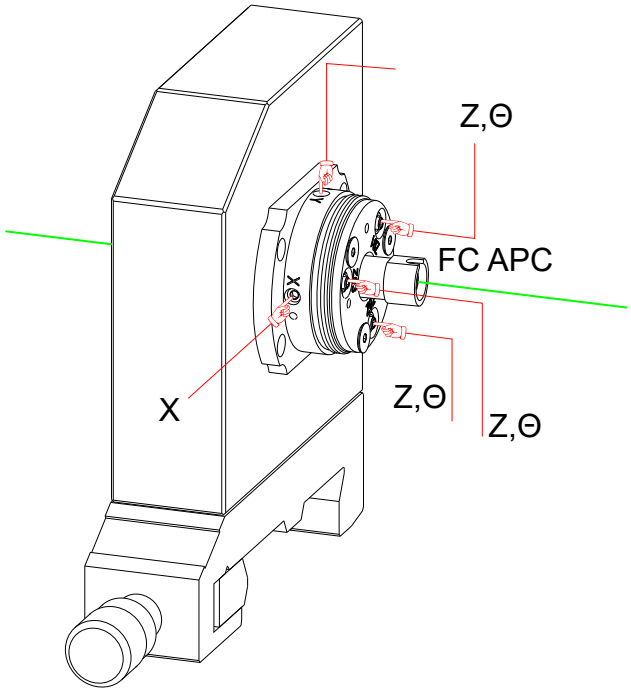

Fig. 30: Fibre port (FP)

To couple the light of the laser into the single mode fibre, we are using an aspheric “FiberPort” collimators with bulkhead of type PAF2-2A which is attached to a mounting plate.

Fig. 31: FibrePort PAF2-2A

For further details for the FibrePort please see here, “4.0 Fibre Port Collimator with bulkhead” on page 21.
To guide the light, we are using single mode optical fibre to ensure that we will have a homogeneously illuminated cross section. Furthermore, the use of single mode fibre removes the need for additional spatial filters when free space light propagation is used. Since we are using a single mode laser, we must make sure, that no back reflected light destroys the single mode. At all optical surfaces more or less strong back reflection takes place, especially at the fibre entrance surface. To avoid the back reflection, we are using ACP (angle physical contact) connectors. The contact surface is declined by an angle of 8°.

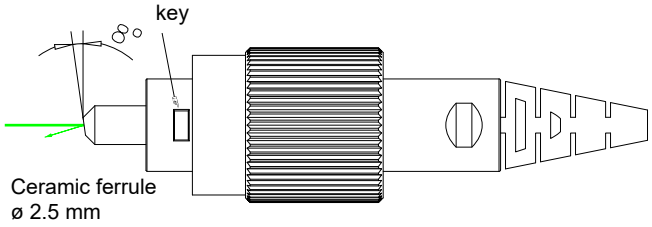

Fig. 32: Angled physical contact connector

The direction of the slant is indexed by a key which slips into the slot of the fibre joint. Connectors with such a key are listed as FC types.

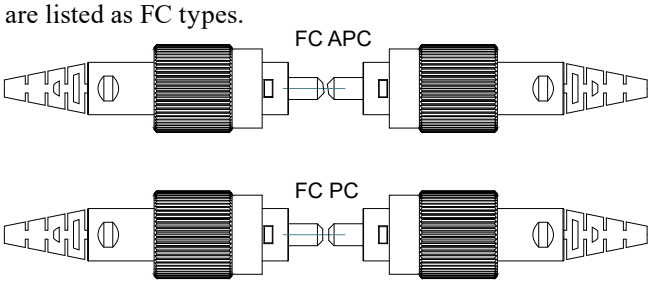

Fig. 33: FC-APC (upper) and FC/PC Patch cable (lower picture)

For the holography we need the object and the reference laser beam, which is created by optically splitting of the initial laser beam.

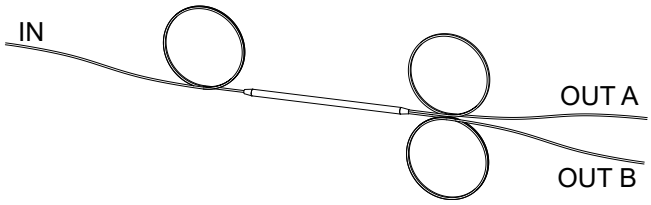

Fig. 34: Single mode fibre splitter 50/50

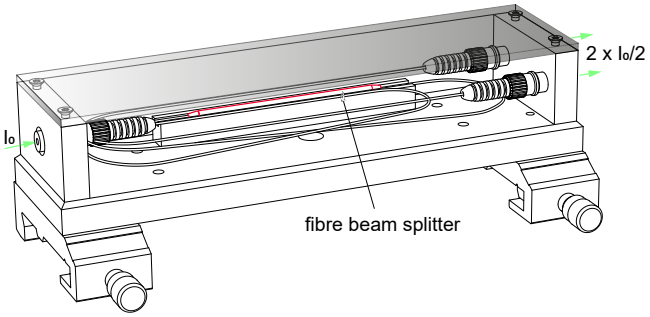

Fig. 35: Single mode beam splitter unit

The single mode fibre splitter is built into a rigid structure to avoid any mechanical stress from the fibres. On the left side (I_0) an FC-APC panel jack the fibre patch cable from the fibre port is connected. On the right side (Fig. 35) the panel jacks for the fibre patch cable of the reference and object light are provided. The beam splitter unit is placed onto the optical rail as shown in Fig. 26.

3.1.3 Beam handling

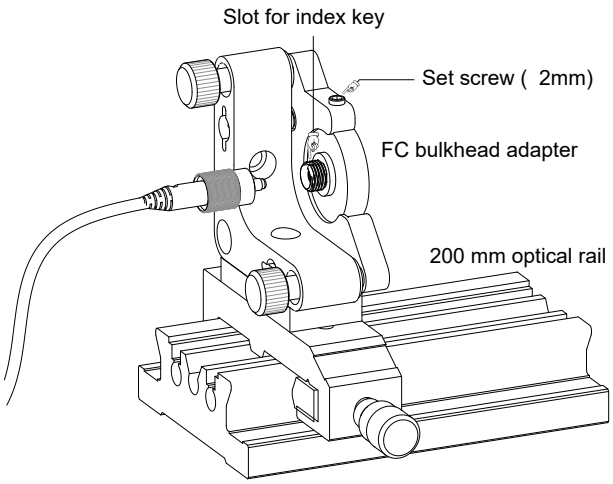

Fig. 36: Fibre optics termination

Each of the two fibre patch cable is attached to a two axis kinematic mount which is attached to an optical rail of 200 mm length. The fibre's FC connector is inserted into the bulkhead adapter. The adapter is fixed to the kinematic mount with a M3 grub screw and can be rotated such, that the slot for the key of the fibre connector is in a suitable position. The adapter of the second kinematic mount should be in the same position to ensure same polarisation.

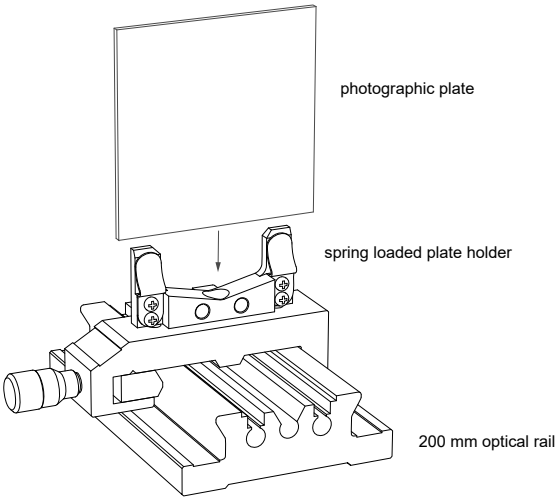

Fig. 37: Photographic plate holder

The holographic plates will be fixed by means of two spring loaded nylon coated clips. The nylon coating helps to prevent damage to the optic being held.

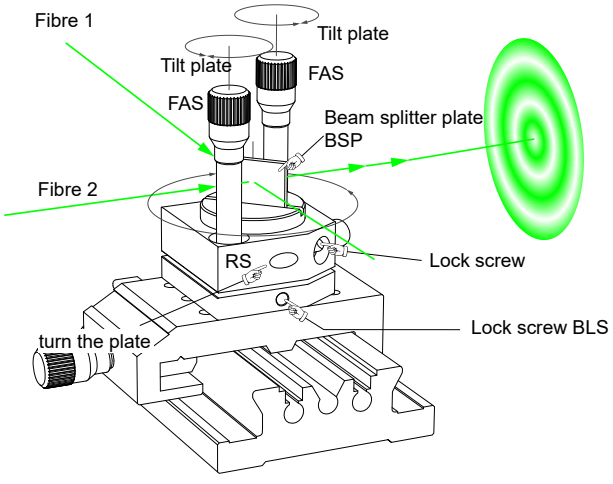

Fig. 38: Interference checker assembly

Prerequisite for successful creation of holograms is the long-term interference and phase stability. With the interference checker the condition of the light source and the environment is checked. The light of the reference light (fibre 1) and the object light (fibre 2) is superimposed by a beam splitter plate. The beam splitting plate (BSP) is mounted into a holder and divides the incoming beams at a ratio of 1:1. The mount is inserted into the adjustment holder and fixed by the lock screw and can be turned around its vertically axis by turning the screw (RS). For this purpose, an Allan key screwdriver is provided. By means of the two fine adjustment screws (FAS) the beam splitting plate can be tilted. The adjustment holder is fixed by means of the lock screw (BLS) to the carrier.

3.1.4 Laser controller and timer DC-0090

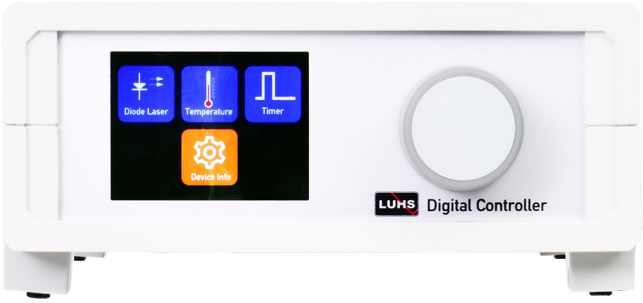

Fig. 39: Front view of the diode laser controller and timer

The diode laser module is connected via the 15 pin HD SubD jacket at the rear of the controller (Fig. 40). The controller reads the EEPROM of the laser diode and sets the required parameter accordingly. The DC-0090 is powered by an external 12 V/1 A wall plug supply. A USB bus allows firmware updates. The central settings knob rotates a precision optical encoder to set the parameter like temperature, injection current and exposition time.
The controller is equipped with a touch panel display and industrial highly integrated circuits for the bipolar Peltier cooler as well as for the injection current and modulation control of the attached laser diode. The injection current is stabilized within ± 1 mA and the diode laser temperature within ±0.01 °C.
The DC-0090 Diode laser controller and timer allows to switch the attached laser on for a limited time with a certain delay. Furthermore, the reading and buttons of the display are turned to red colour before and during the exposure time to avoid undesired light which may affect the intended illumination.

Fig. 40: Rear view of controller DC-0090

When the external 12 V is applied and the controller switched to ON, the controller starts displaying the screen as shown in the figure below.

Fig. 41: Start screen

During start-up, the controller checks the presence of the diode laser module and reads its parameter. After that, the controller is ready and touching the screen brings up the PIN authentication menu.

Laser Safety

The first interactive screen requires the log in to the device since due to laser safety regulations unauthorized operation must be prevented. In general, this is accomplished by using a mechanical key switch. However, this microprocessor operated device provides a better protection by requesting the entry of a PIN.

Fig. 42: Password entry screen

After entering the proper key, the next screen is displayed, and the system is ready for operation.
On the main screen the buttons for the control of the diode laser and its temperature as well the exposition timer are located. An additional button provides information of the attached laser diode.

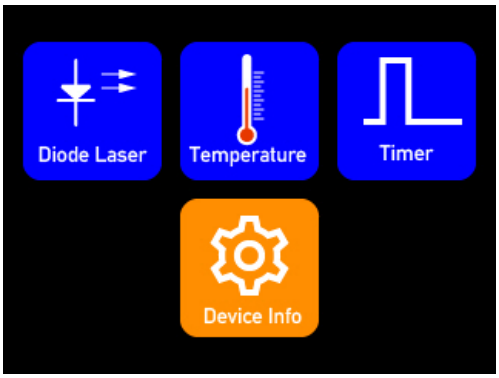

Fig. 43: Main Screen

After touching the "Diode Laser" button, the following screen appears.

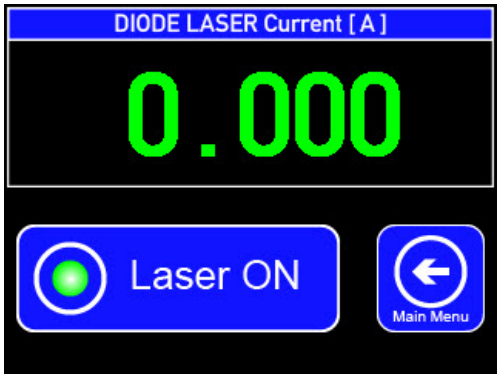

Fig. 44: Injection current settings

By turning the setting knob, the desired injection current is selected and displayed. The maximum current is limited to the value stored in the EEPROM of the attached laser diode module.

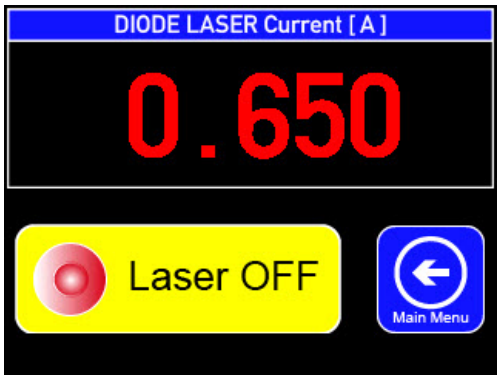

Fig. 45: Laser ON/OFF

By touching the "Laser ON/OFF" button, the laser diode is switched accordingly. The colour of the injection current switches from green to red and the laser button to red on yellow. Touching the "Main Menu" button brings back the main menu screen.
Touching the "Temperature" button on the main menu screen (Fig. 40) activates the temperature setting page.

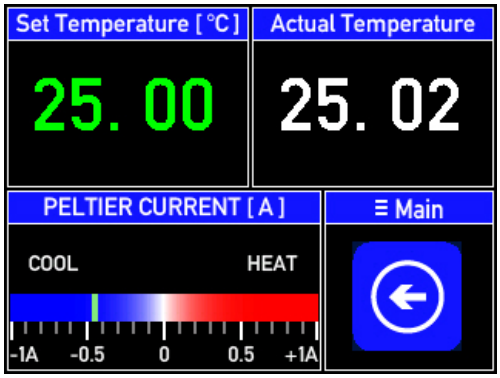

Fig. 46: Temperature settings of laser diode

The set temperature is displayed in green colour and can be set by turning the settings knob. Furthermore, the actual current of the Peltier element is shown in such a way, that cooling, or heating of the element can be observed.
Touching the "Timer" button on the main screen brings up the exposition screen. All elements are coloured to red since the holographic film plate is not sensitive to this wavelength (Fig. 47).

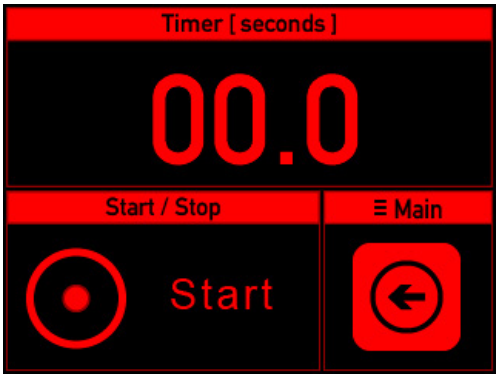

Fig. 47: Timer settings

By turning the settings knob, the exposition time is set in seconds. Either touching the “Start” button or pushing the settings knob switches on the laser. The countdown is shown and after reaching the selected exposition time the laser is switched off.

Fig. 48: Timer settings

The exposition can be stopped by either pushing the settings knob or touching the “Stop” button.

3.2 Preparation and development equipment

The required chemicals are provided in sealed plastic bottles. The quantity is sufficient for 4 litres of developer and bleacher.

For the development of the holograms and preparation of the developer chemicals the following items are provided:
1. Five dishes, one for the developer, one for the stop bath, one for the bleacher, one for the washing and one for the washing with wetting agent.
2. Two one litre bottles, one for the SM-6 developer and one for the Amidol bleacher.
3. By means of the balance (accuracy 0.1 g) and spatula the chemicals are exactly portioned in accordance with the given recipe (see “Table 1: Chemistry receipts” on page 15).

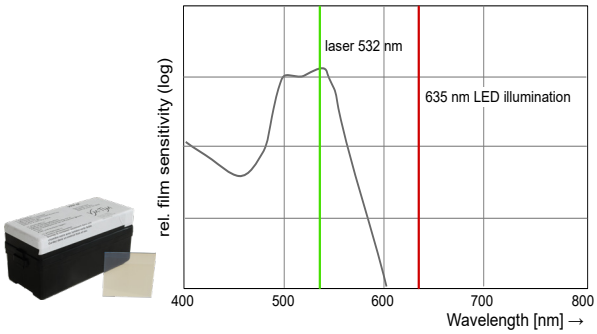

Fig. 49: Sensitivity curve of VRP-M holographic plates VRP-M Holographic plates

The VRP-M emulsions may be used equally well with pulsed lasers and with cw radiation.
White-light holograms made on VRP-M have a natural green reconstruction colour. The spectral sensitivity of the emulsion is ideally suited to use the radiation of 532 nm which is available from DPSS laser with frequency doubling. The plates have a size of 63 x 63 mm. As can be seen from Fig. 49 the emulsion is not sensitive in the red and a LED with 635 nm can be used as dark room illumination without effecting the exposition process.
The box should only be opened in a dark room. The side coated with the emulsion is slightly sticky and can be identified by touching.

3.3 Chemicals processing instruction

It is important to follow good laboratory practice while processing. Wipe up any spillage as soon as it occurs and use the polythene gloves. The working temperature of all chemical solutions described below should be 20 ± 2°C.

3.3.1 Chemistry preparation

First of all, you will need to prepare the developing and bleaching solutions. After preparation you can store these solutions in the closed bottles for three days. The receipts below are given for 1 litre of each solution. In one litre of ready developer there is possible to process 300 plates of the VRP-M film (plate’s dimensions 63x63mm). If you are expecting to process less film in one session, please reduce the quantity of the chemicals accordingly.

Chemical	*Formula*	*g/litre*	*dilution order*
Developer SM-6			
Sodium Hydroxide	NaOH	12.0	1
Phenidone	C_6H_5-$C_3H_5N_2O$	6.0	2
Ascorbic Acid	$CH_2OHCHOH$ (CHCOH:COHCOO)	18.0	3
Sodium Phosphate (dibasic)	Na_2HPO_4	71.6	4
Water (distilled)	H_2O		to 1.0 Litre
Bleach PBU-Amidol			
Potassium Persulphate	$K_2S_2O_8$	10.0	1
Citric Acid	$HOC(COOH)(CH_2COOH)_2$	50.0	2
Cupric Bromide	$CuBr_2$	1.0	3
Potassium Bromide	KBr	20.0	4
Amidol	$(NH_2)_2C_6H_3OH•_2HCl$	1.0	5
Water (distilled)	H2O		to 1.0 Litre

Table 1: Chemistry receipts

For each solution preparation take ~0,6 litre of distilled water at the temperature of ~45°C. Dilute chemicals in the order given above. Add distilled water to obtain 1 litre of each solution.

3.3.2 Prepared solutions storage

The developer's solution remains developing properties while stored in dark room conditions for three days.
Bleaching solution can be stored in dark room conditions for about one month.
Processing even one film in the developing and bleaching solutions noticeably reduce their lifetime.
All solutions should be stored in the closed glass or non-active plastic bottles in a room temperature and darkness.

3.4 Processing of the exposed film

1. Fill the separate development trays with the developer, bleach and distilled water for washing (two trays for water).
2. Switch the room lights off and the safelight on (red LED).
3. Put the exposed film into the developing tray (containing SM-6 developer) with its emulsion side towards the inside.
4. Agitate the developer for 2 minutes. Film should become dark.
5. Put the developed film in the one of the trays filled with distilled water and agitate it for 2 minutes for wash out the developer.
6. Switch the room lights on, as the film is no longer sensitive to light
7. Put the developed and washed film in the tray containing the bleach and agitate it for 2-3 minutes, until the film turns from the dark to clear. After the film becomes clear, agitate it in bleach for 2 minutes more.
8. Put the bleached film in the another tray with distilled water and agitate for 5 minutes to wash out the bleach.
9. Put the washed film in the next tray with distilled water with wetting agent (Agepon) and agitate for 1 minute (simple way to prepare water with wetting agent is to put just one drop of commercially available dish washing cleaner (such as Fairy, or similar)).
10. Place the film, emulsion side up on the absorbent mat (paper towel). Carefully wipe water from the emulsion surface using a folded tissue. Turn the film over and wipe the film base side. Turn the film over again and wipe the emulsion with a fresh tissue. Ensure that no water drops remain on the film.
11. Now you can dry the film in two ways:
    → hang it and wait till it will dry up,
    → use a hair drier and dry it quicker. For that hold the film in the palm of your hand emulsion side up and dry it with a hair drier (maximum setting 1 KW) placed about 30 cm away. This should take about 1 minute. (Note that hot film will have a different replay colour than that at the room temperature

3.5 Basic alignment

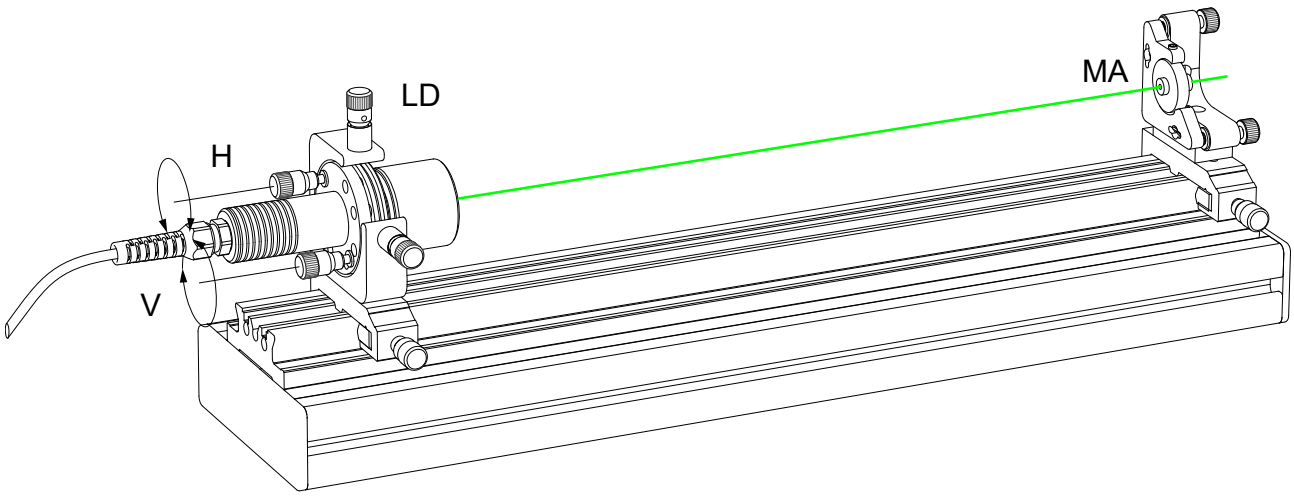

The laser diode and one of the kinematic mounts (MA) is placed onto the rail. With the H and V adjustment screw the laser beam is aligned such, that it passes undisturbed the hole of the fibre bulkhead of MA.

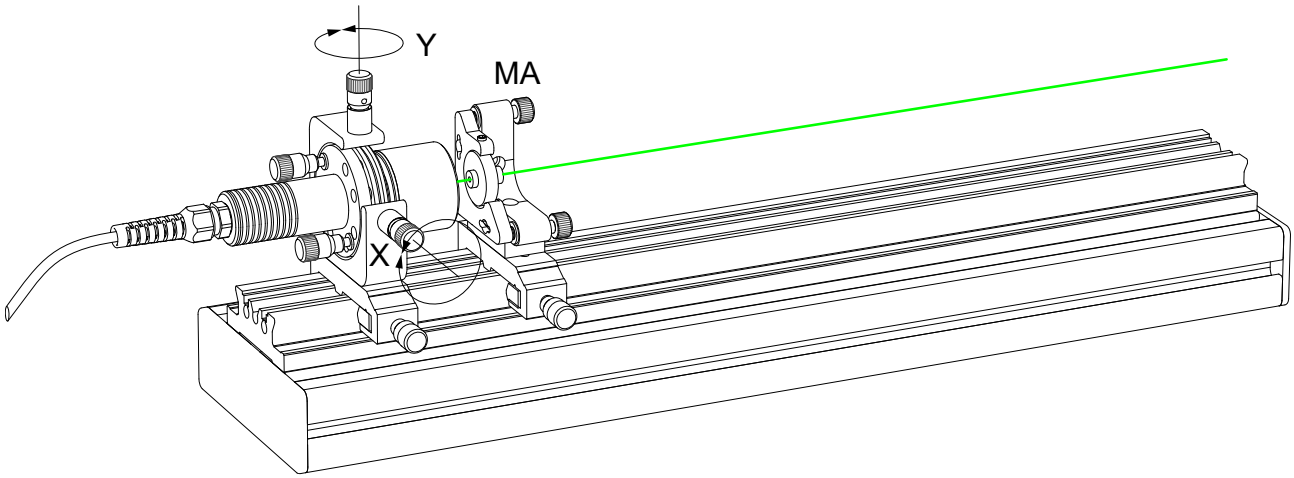

The MA is moved towards the laser diode as close as possible. With the X and Y adjustment screws the laser beam is aligned in the same way. Then MA is moved back and with the H and V screw adjusted again. This process may be repeated several times until the beam is perfectly parallel to the mechanical axis of the rail.

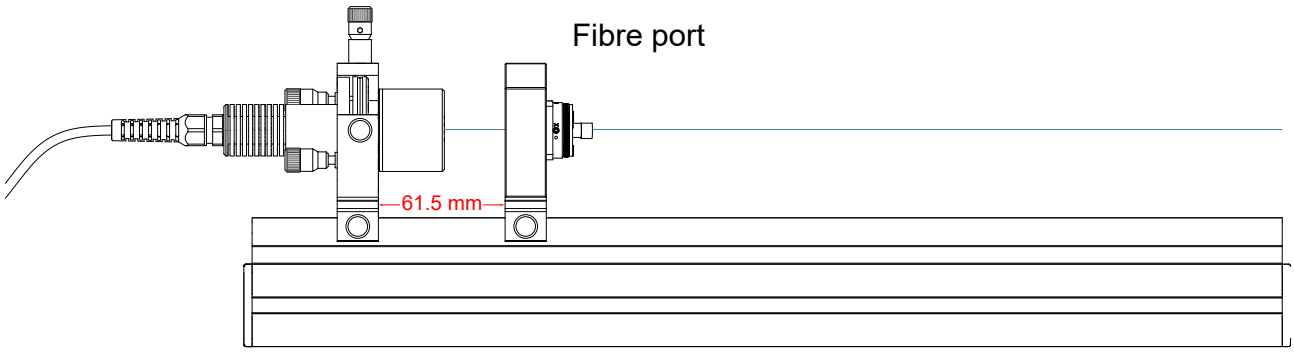

Once the alignment of the laser beam is done, the fibre port is placed onto the rail. The distance between the laser diode and the fibre port must be 61.5 mm as shown above. This distance is only relevant, when the z position of the focusing lens inside the fibre port has not been misaligned (see also the instruction “4.2 Zθ Adjustment” on page 21).

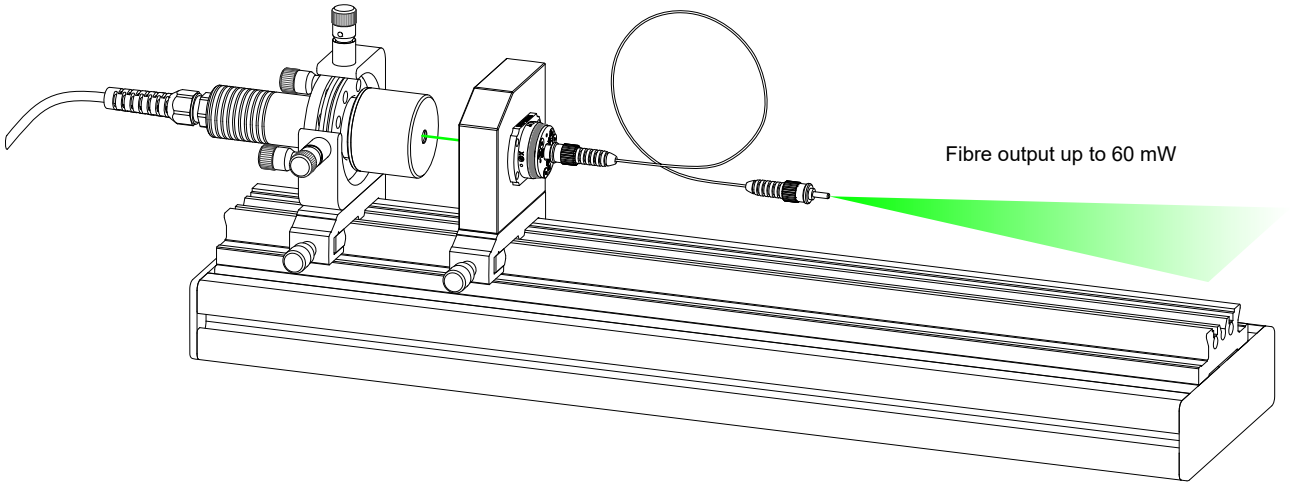

The fibre patch cable with the 900 µm buffer is connected to the fibre port. The output power can beched on a piece of paper, however it would we of help to use a power meter. With a mediocre alignment the fibre emits already 25-30 mW. Gently align the H, V, X and Y screws of the laser diode and finally also the X and Y screw of the fibre port using the provided 1.3 mm Allan key with rounded head.

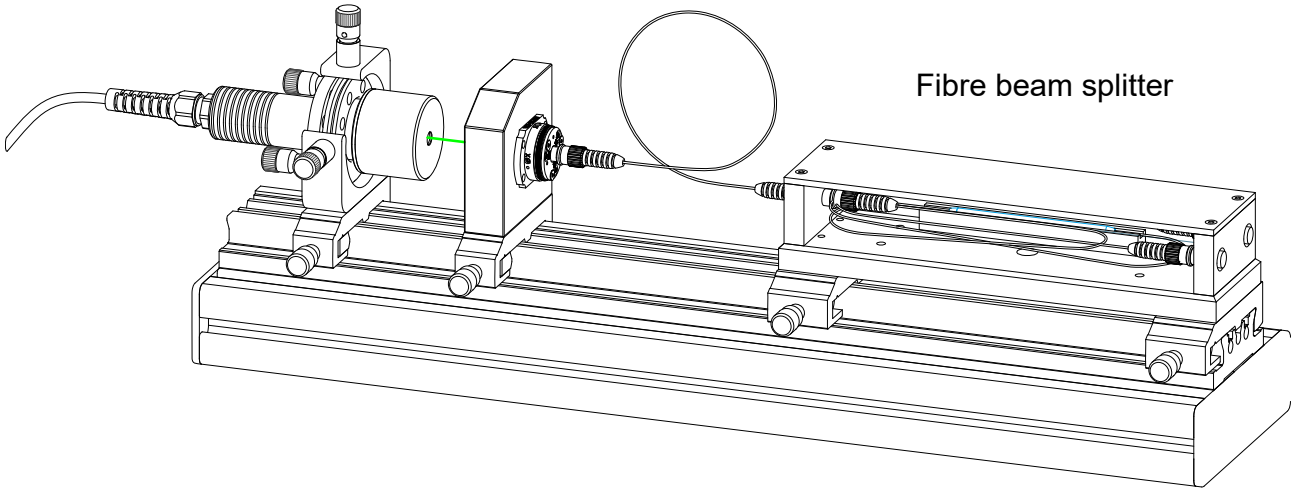

After optimising the fibre output, the fibre beam splitter is placed onto the rail.
Note:
In case the laser light which leaves the fibre sidewards as cladding modes disturbs the exposition of the film plates, a black cloth is provided which is placed on top of the fibre port and fibre beam splitter (not covering the laser diode).

3.6 Set-up for stability check

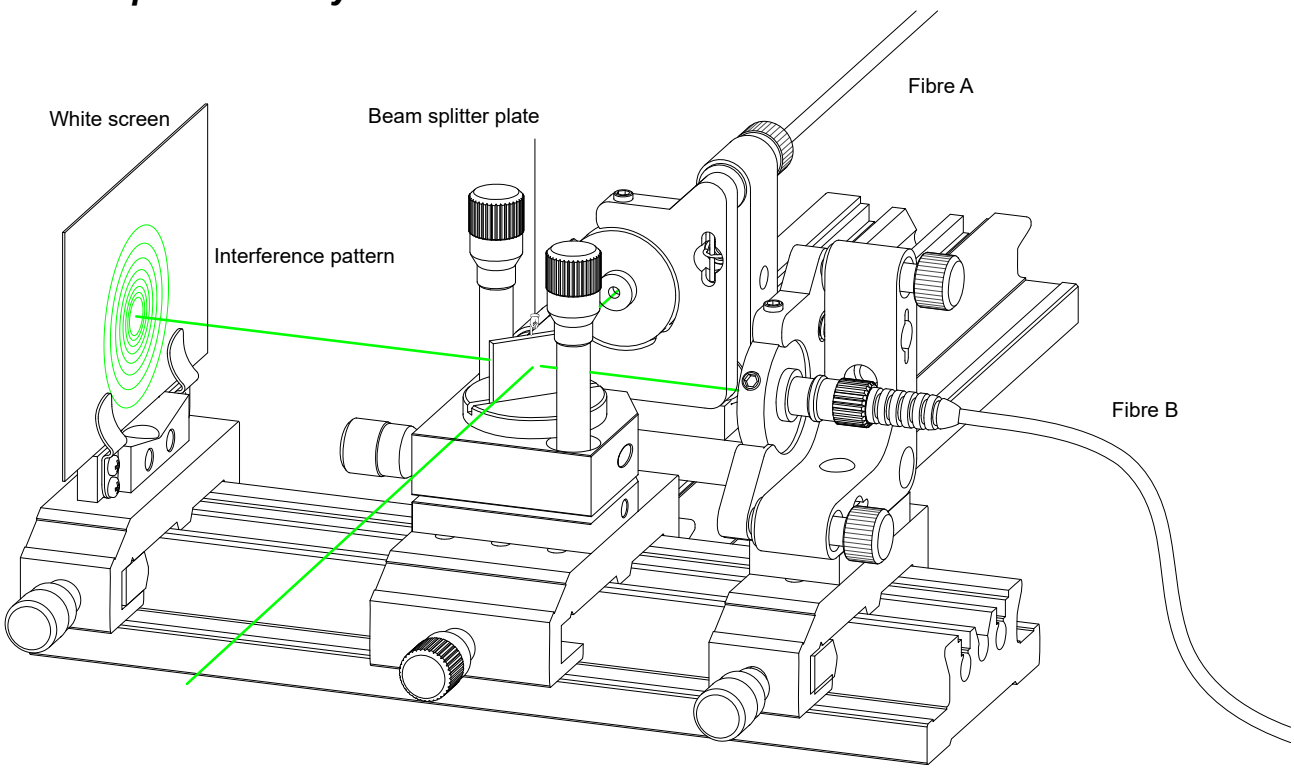

Fig. 50: Set-up for stability check

This setup shows two important things, the interference, and the stability of the interference fringes. For this purpose, the reference beam and the object beam (either coming from Fibre A or Fibre B) are superimposed by using a beam splitter plate.
The set-up is arranged in such a way, that a Michelson interferometer results, however without mirrors. The interference pattern is observed on a piece of white chard inserted into the film plate holder. The fringes should not move or dither during a time of about 60 seconds. In this case the environment is quiet enough and suitable for holographic recording.

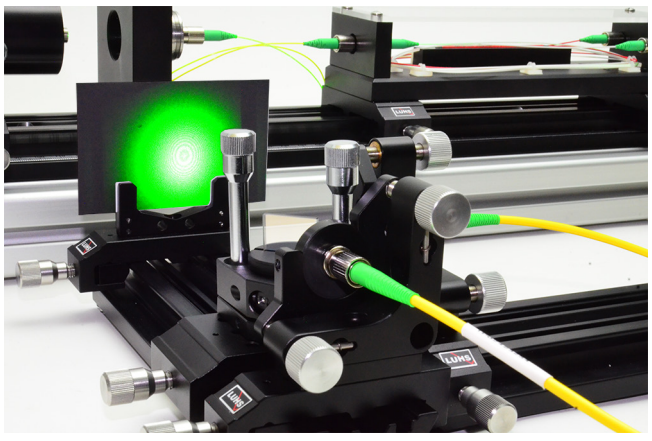

Fig. 51: Observation of interference fringes

Please note:
In this setup we superimpose two strongly divergent beams, and the resulting fringe pattern is different from what we know from a Michelson interferometer, where almost parallel beams are superimposed. It is important that the fibre faces where the beams are emerging should have the same distance to the superimposition location (beam splitter plate).
Otherwise, two spherical waves with different diameter and radius of curvatures are overlapping and the fringes might not been seen.
With the adjustment screws, the direction of the reflected beam is aligned with respect to the transmitted beam, so that the interference pattern is centred on the screen.

3.7 Recording of a transmission hologram

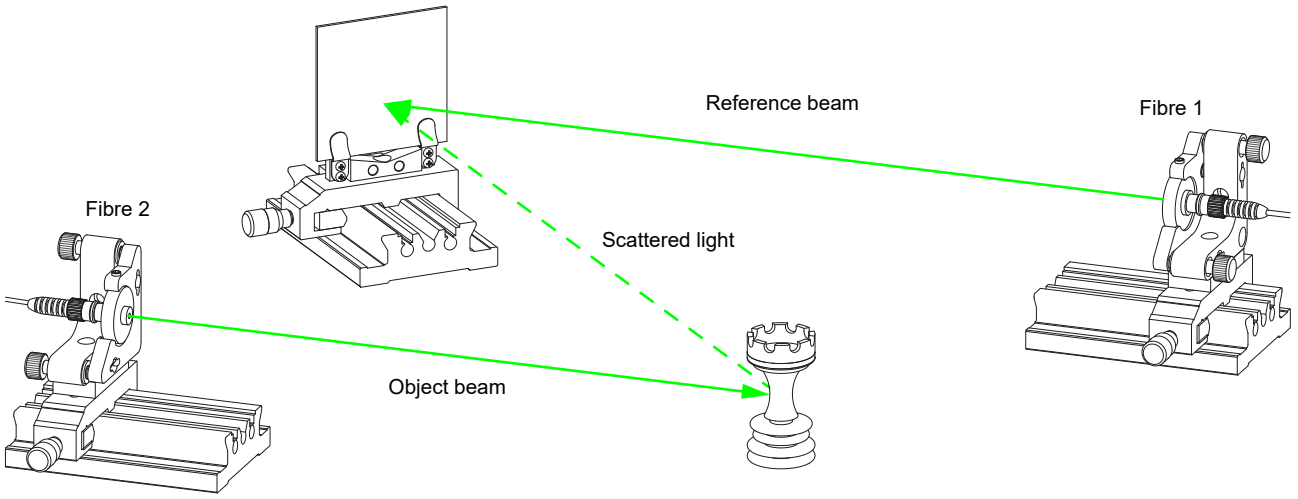

Fig. 52: Set-up for transmission hologram

We start with the setup for the creation of a transmission hologram as shown in Fig. 52.
In the following step the object is placed into the setup in such a way that most of the scattered light hits the holographic plate. A piece of paper with the size of the plate can be used as alignment aid.
The holographic plate is illuminated from the scattered light emerging from the object and the reference beam.

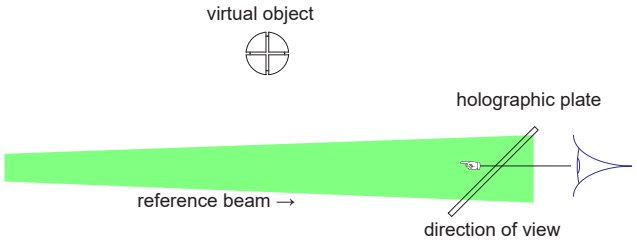

Fig. 53: Reconstruction or viewing of the hologram

For the reconstruction or observation of the hologram a laser beam like the reference beam is required. One looks through the plate which is illuminated from the back side by the reference beam of the setup. One will notice the virtual object after a moment of eye adaptation.

3.8 Set-up for the creation of a Denisyuk hologram

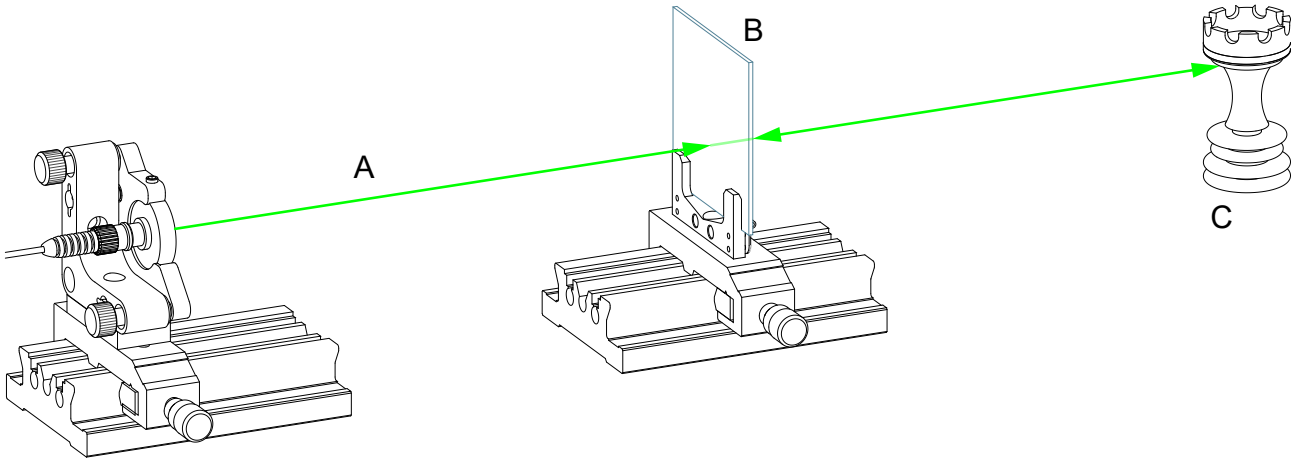

Fig. 54: Set-up for a Denisyuk hologram

For the arrangement after Denisyuk only one beam is used which makes the set-up even more simple. The beam (A) of one fibre shines through the holographic plate (B). The transmitted light is scattered from the object (C) to the holographic plate where the interference pattern is recorded.
The development of the plate is processed in the same way as for the transmission hologram.
A particularity of the Denisyuk holograms is the ability to be viewed by the illumination with a white light source.

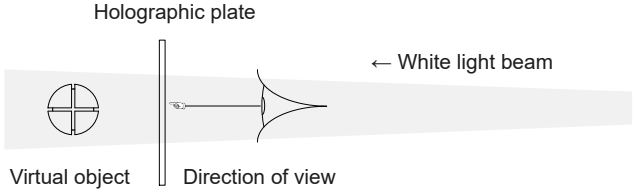

Fig. 55: Reconstruction or viewing the hologram

3.9 Set-up for a reflexion hologram

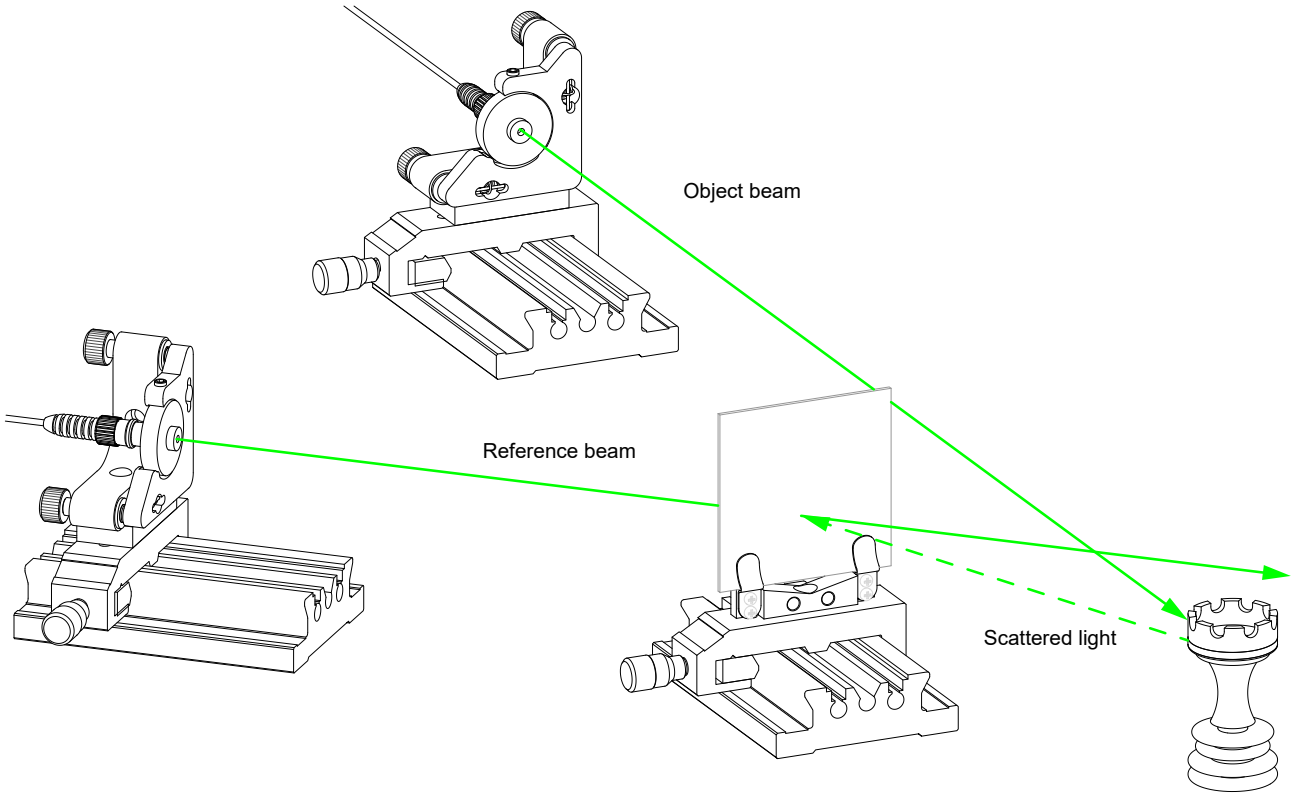

Fig. 56: Set-up for reflexion hologram

Another possibility for creating a reflexion hologram is the use of two beams compared to the Denisyuk method. The object is illuminated by the strong object beam whereas the reference beam illuminates the holographic plate. Inside the emulsion the created interference structure is stored, and holograms of this type can also be viewed under white light illumination.

4.0 Fibre Port Collimator with bulk-head

Fig. 57: PAF2 Series Aspheric FibrePort Collimators with Bulkheads

4.1 Mechanisms of the FibrePort

The FibrePort is a fibre collimator and coupler with six degrees of freedom (5 axes, plus rotation). It uses a movable lens as the alignment mechanism while holding the fibre stationary. This provides an extremely stable and repeatable platform forcoupling and collimating. All adjustments are coupled.

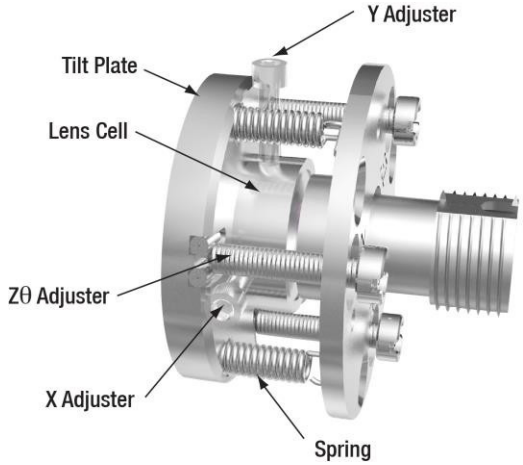

Fig. 58: The Internal Mechanism of a FibrePort

The FibrePort consists of a body, a magnetic lens cell (MLC) adhered to a tilt plate, and a bulkhead with fibre connector. The bulkhead is locked onto the FibrePort body by three flat head screws and the clamp plate. By loosening the flat head screws, the fibre bulkhead can be rotated freely and can be used to coarsely alignthe bulkhead with polarization maintaining fibre.

4.2 Zθ Adjustment

The MLC is adhered to the tilt plate, which can be translated in the Z direction via equal adjustments of the three adjusters. These adjusters consist of three ball-end fine adjust screws labelled Zθ1, Zθ2, and Zθ3 which ride in ceramic ball seats. The hardened steel ball-ends and ceramic ball seats are attached with a high- temperature, low-outgassing epoxy to provide a stable, long-wearing kinematic system. The extension springs provide counter force against the fine adjust screws. The Z (optical axis) translation range is ±1.0 mm.

4.3 X-Y Adjustment

The MLC can be translated in X-Y using the socket head cap screws (SHCS) in the side of the FibrePort body. The MLC rests on a leaf spring, and the X-Y screws push the cell against the leaf spring. The X-Y adjusters are stabilized by 0-80 setscrews with a 0.028” hex removing backlash. These setscrews, accessible from the top of the FibrePort, can be used to tune the feel of the X-Y screws. A third SHCS behind the leaf spring can be used for locking. The travel range of the aspheric lens in the X and Y directions is ±0.7 mm; in most cases when the FibrePort is used in a standard collimation/coupling application, only a small portion of this translation range is needed.

1.1. Location of Screws on the FibrePort

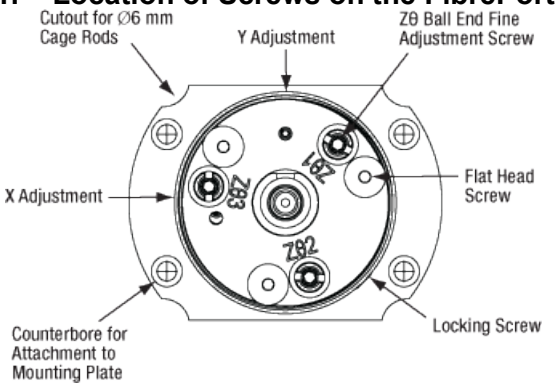

Fig. 59: Figure 2 Location of Screws on the FibrePort

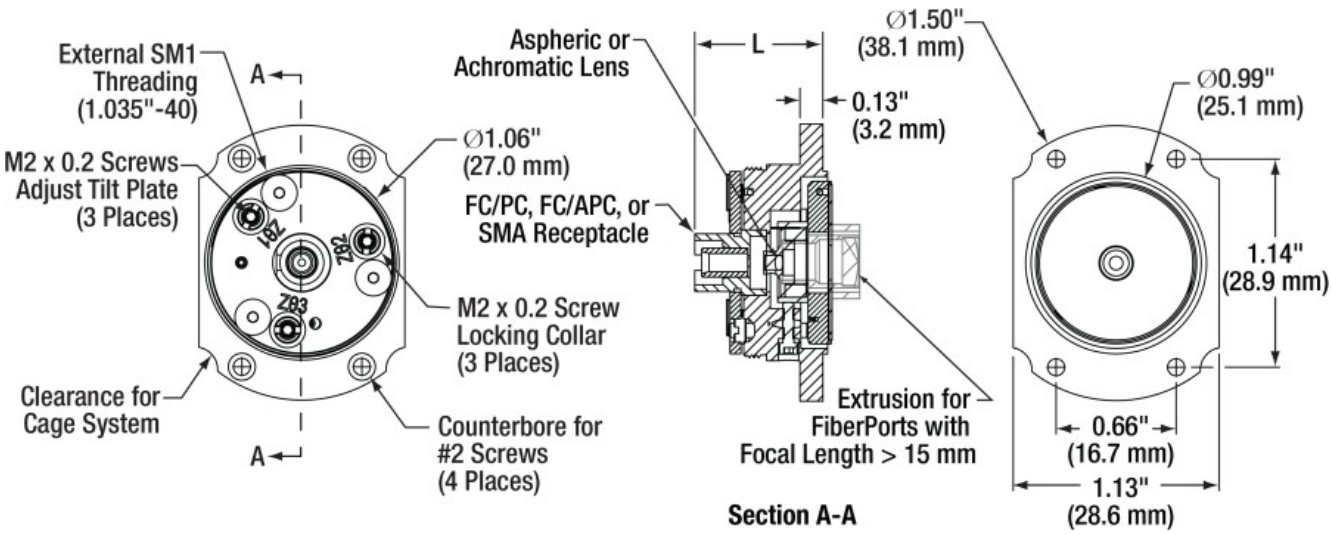

Fig. 60: Figure 3 Schematic Diagram of the FibrePort

CAUTION

Most applications DO NOT require locking.

4.4 Pre-Alignment

Note: A new FibrePort comes pre-aligned with no additional pre-alignment necessary for collimation. Each FibrePort is aligned for the wavelength that is specified in its mechanical drawing, available on the web. The following instructions should be followed if the FibrePort has been adjusted since purchase, or if you are operating under different conditions than the intended collimation provides (such as a different input wavelength than the factory alignment). Before attempting to collimate or couple fibre with your FibrePort, it is crucial to ensure that the FibrePort is properly aligned. If your FibrePort has been adjusted since purchase, please follow the steps below to provide the best performance.

4.4.1 Aligning the Tilt Plate

With the laser off, centre the lens by eye in the tilt plate aperture by turning the X and Y adjustment screws. Turn the Zθ adjusters counter-clockwise until the tilt plate is flat against the FibrePort body and orthogonal to the beam axis. This must be done fairly precisely and can be achieved one of the following ways:

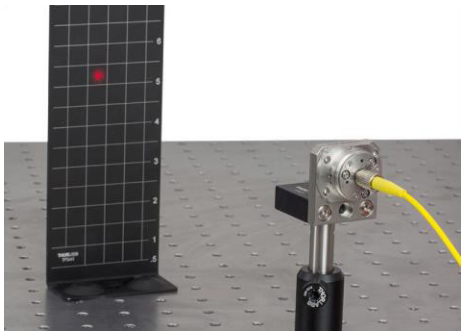

Fig. 61: Aligning the Tilt Plate by Utilizing an Alignment Grid

4.4.2 Using Input Laser (Recommended)

1. Securely mount the FibrePort so it does not move during alignment.
2. Turn the Zθ adjusters counter-clockwise until it is clear that they are no longer translating the tilt plate.
3. Insert a visible fibre laser.
4. Aim the beam at an alignment screen.
5. Turn each Zθ adjuster clockwise until the beam position is affected. Once each adjuster has just begun to affect position, the adjusters are in contact with the tilt plate. If done carefully, the tilt plate is still flush against the body of the FibrePort and is orthogonal to the optical axis.

4.5 Coupling into a Fibre

4.5.1 Principle

While translation in the X-direction and Y-direction can be directly made by using their respective adjusters, translation in the Z-direction must be made by incremental tip/tilt adjustments. As a result, the beam's path as the adjusters are turned may not be intuitive. Equal rotations to each of the Zθ adjusters result in the beam spot tracing a triangle around the core of the fibre, as illustrated below. Once some measureable output exists, a typical alignment strategy would consist of turning each screw to maximize the output, and then continuing to turn slightly beyond maximum (about 95% of your local max). The maximum seen in passing will continue to increase until lens-to-fibre spacing is optimised (spot size is minimized). This strategy has the effect of translating the beam in a triangle of decreasing width with each set of adjustments. The beam's path is shown with the point of view of the fibre that is being coupled into.

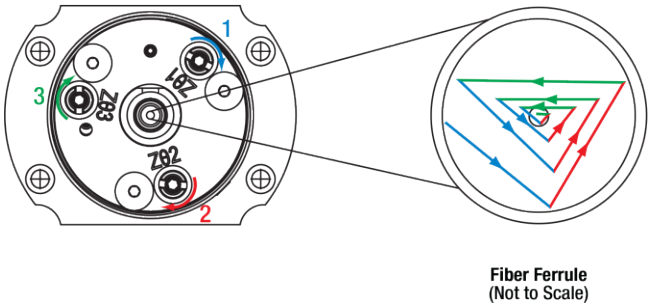

Fig. 62: When turning each Zθ adjuster by equal increments, the beam traces a triangular pattern of changing width.

The maximum power is seen not at either end of each turn's

travel range, but in the middle when the beam is closest to the fibre's core.

Note that the typical maximum coupling efficiency is highly dependent on the system configuration and setup. A perfect system and setup can yield efficienciesup to ~90% with fibres that are not AR coated. Slight system alignment error and/orless than ideal system components that are common in most configurations make70% - 80% coupling efficiency the typical value. Efficiencies below 50% may indicate significant component mismatch or alignment error.

4.6 Fibre Coupling

6. Start with a pre-aligned FibrePort, as discussed in Chapter 4. With the system turned on, the laser should be visible through the connector end of the FibrePort (if using a visible laser).
7. Insert a multimode (MM) fibre that is compatible with your system. Plug the fibre that is being coupled into a power meter. First maximize the X and Y positions by adjusting the X and Y adjusters and observing where the intensity peaks for each position. If large adjustments (>1 turn) are necessary, check incoming beam alignment. Once a maximum is reach, these adjusters should not be changed unless SM fibre is later used.
8. Turn each Z adjuster clockwise to maximize the output, then continue to turn slightly beyond maximum (to about 95% of your local maximum). If turning an adjuster clockwise decreases output, skip that adjuster for that round of adjustments. Repeat.
9. Once the local maxima values begin to decrease, reverse the direction, and turn each adjuster to maximize the output, and not beyond.
10. If coupling into a SM fibre, exchange the MM fibre with a SM fibre. The intensity measured by the power meter will likely drop significantly.
11. Repeat Steps 3 and 4. The adjustments will be smaller and more sensitive. If adjustment of all screws in either direction lowers the output, the beam spot may be centered on the fibre core, but improperly focused. Turn each adjuster a small amount (1/8th turn) in the same direction, then maximize each Zθ adjuster. If the new maximum is lower than the previous, turn each Zθ adjuster a small amount in the other direction and maximize. Repeat until absolute maximum is found.
12. (Optional) If desired, the adjusters can be locked via the locking collars by the use of the included SPW403 spanner wrench. Additionally, the lens cell can be locked in place by installing the included 0-80 screw located in the 4:30 position of the front face of the FibrePort. See Chapter 8 for detailed instructions.

4.7 Locking the FibrePort

If you are leaving the FibrePort on a table, it does not need to be locked. Typically, an aligned FibrePort can be hand carried and moved without causing alignment changes. The locking process can cause a shift in the alignment of the FibrePort. For situations where the FibrePort might undergo large vibrations or shock, such as shipping, we recommend locking or potting the FibrePort. Locking the FibrePort is an iterative process requiring patience. The locking screw pushes the lens cell firmly against the X and Y screws. If the locking screw is tightened too quickly, the alignment of the FibrePort magnetic lens cell (MLC) will be shifted.

When locking the position of the MLC using the procedure below, monitor the position of the beam if the FibrePort is being used as a collimator. If the FibrePort is being used to couple light into a fibre, attach a suitable optical detector to the output end of the fibre and monitor the output signal of the detector during the locking process. In either case, make sure that the locking process does not change the alignment of the MLC.

13. Carefully thread the small locking screw into the FibrePort at the 7:30 o'clock position on the outer diameter.
14. As you slowly tighten the locking screw, adjust the X-Y screws as required to maintain the alignment. DO NOT torque down any of the screws. Applying too much pressure with the screws can permanently damage the magnet/lens assembly, the 0-80 screws, and/or destroy the alignment. When the X,Y, and locking screws are just snug, the lens is locking in place.
15. To prevent accidental changes with the Zθ adjusters, carefully tighten the locking collars with the spanner wrench (Item # SPW403) while holding each adjuster with the 0.050" hex key/ball driver. Make minor adjustments to the adjusters as necessary to maintain the alignment of the MLC. DO NOT torque down any of the screws.
16. If optimal alignment is lost when locking, first loosen the locking collars ½ turn, then loosen the adjuster screws ¼ turn each. The less the locking collars have to travel to be locked, the better. Now adjust the X- Y screws to regain optimal alignment. Repeat Steps 2 and 3.